Journal of Sound and Vibration (1997) **207**(2), 207–226

NON-LINEAR DYNAMICS OF AN ELASTO–PLASTIC OSCILLATOR WITH KINEMATIC AND ISOTROPIC HARDENING

M. A. Savi

Department of Mechanical and Materials Engineering, *Instituto Militar de Engenharia*, 22.290.270—*Rio de Janeiro—RJ*, *Brazil*

AND

P. M. C. L. Pacheco

Department of Mechanical Engineering, *CEFET/RJ*, 20.271.110—*Rio de Janeiro—RJ*, *Brazil*

(*Received* 5 *August* 1996, *and in final form* 14 *April* 1997)

This contribution reports on a dynamic analysis of an elasto–plastic oscillator. Kinematic and isotropic hardening are considered. The equations of motion have five state variables associated with complementary conditions. System dynamics is treated by performing a split in phase space in two parts. This split is suggested by an analysis of the equations of motion near equilibrium points and permits conclusions about high dimensional dynamical system by analyzing subspaces with lower dimension. This physical consideration is in close agreement with the operator split technique used for the numerical solution. Some numerical results are shown for free and forced vibrations of the oscillator with kinematic, isotropic and kinematic/isotropic hardening.

1. INTRODUCTION

The elasto–plastic behavior describes the deformation mechanisms of most metals and alloys at room temperature. The theories of elasticity and plasticity are both based on experimental studies of stress-strain relations in polycrystalline aggregate under simple load conditions. Elasto–plasticity theory describes the well known behavior of bodies that present an elastic reponse until a limit, defined by the yield surface, is reached. After this limit, the body presents a plastic response which is associated with irreversible strains.

The hardening effect represents the way of how plastic strains modify the yield surface. It is a normal situation and can occur in many different ways, depending specifically on the material considered. There are many idealized models to describe this phenomenon. A great number of situations can be properly represented by a combination of kinematic and isotropic hardening. Kinematic hardening is characterized by the translation of the yield surface. Isotropic hardening corresponds to a uniform expansion of yield surface. The understanding of elasto–plastic behavior is important in many engineering problems, structural integrity and mechanical conformation being examples. This contribution reports on a dynamic analysis of an elasto–plastic oscillator with kinematic and isotropic hardening. Simple constitutive equations are considered to describe the elasto–plastic behavior. Despite the deceiving simplicity of the model used, its non-linear dynamic response may represent the qualitative response of elasto–plastic structures.

0022–460X/97/420207 + 20 $25.00/0/sv971078

The oscillator equations of motion have five state variables associated with complementary conditions. System dynamics can be treated performing a split in phase space in two parts. One part is called phase plane and includes displacement and velocity. The other part is the internal variables space and includes plastic displacement and internal variables associated with kinematic and isotropic hardening. The proposed split is suggested by an analysis of the equations of motion near equilibrium points. This physical consideration is in close agreement with the operator split technique used for the numerical solution and permits one to analyze a high dimensional dynamical system from subspaces with lower dimension. With these assumptions, a numerical method is developed using an integration scheme associated with the so-called return mapping algorithm. Some numerical results are shown for free and forced vibrations of the oscillator with kinematic, isotropic and kinematic/isotropic hardening.

2. ELASTO–PLASTIC MODEL

Elasto–plasticity theory describes the behavior of bodies that, when subjected to a load P, present an elastic response until the elastic limit, defined by the yield surface, is reached. After this limit, the body has an irreversible response which is associated with plastic displacements [1]. The hardening phenomenon, observed on most metals and alloys, can be represented by a combination of kinematic and isotropic hardening.

Figure 1 shows qualitative plots of elasto–plastic behavior with kinematic and isotropic hardening. Consider a load history imposed on the body. By increasing the load from the origin of the force–displacement space, there is an elastic domain until the limit P_y is reached (point A). Outside the elastic domain, irreversible plastic displacement begins to occur. Displacement continues to increase until point B is reached. At this instant, load begins to decrease and the body presents an elastic reponse. Point C shows the residual displacement imposed by this load process. If the load continues to be decreased, the body keeps presenting an elastic response until the new elastic limit is reached (point D). This limit was altered by the load history. Kinematic hardening requires that the yield surface conserves its original size while it varies its position, whose center is originally at the point O (Figure 1(a)). Isotropic hardening, on the other hand, requires that the yield surface expands but conserves its original center which is initially at the point O (Figure 1(b)). Point D represents the new position of the yield surface limits for both cases.

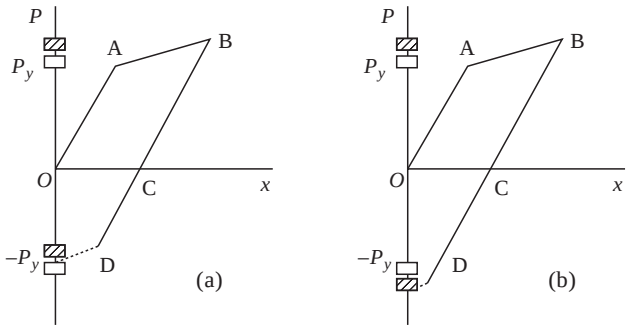

Figure 1. Load-displacement curves for an elasto-plastic body. (a) Kinematic hardening, (b) isotropic hardening.

A constitutive model to describe this elasto–plastic behavior is considered assuming an additive decomposition, i.e., the total displacement, x may be divided into an elastic part, x^e, and a plastic part, x^p. Hence, the force–displacement relation is given by

$$P = K(x - x^p), \tag{1}$$

where K is a stiffness parameter.

The isotropic hardening is described by introducing an internal variable, α, referred to as the *internal hardening variable*. A simple evolution equation of this variable considers that the hardening is linear in the amount of plastic flow, $\dot{x}^p$, and independent of the sign of this flow, sign $(\dot{x}^p) = \dot{x}^p/|\dot{x}^p|$ [2]. This may be expressed by

$$\dot{\alpha} = |\dot{x}^p|. \tag{2}$$

The kinematic hardening is described by introducing a new internal variable, β, referred to as the *back load*. An evolution equation of the back load is defined by means of Ziegler's rule [2]:

$$\dot{\beta} = H\dot{x}^p, \tag{3}$$

where H is a kinematic hardening parameter.

Experimental observations establish that plastic displacement has the following evolution equation [2]:

$$\dot{x}^p = \gamma \text{ sign } (P - \beta), \tag{4}$$

where γ represents the rate at which plastic displacements take place.

The yield surface, which defines the elastic domain limit, is expressed by

$$h(P, \alpha, \beta) = |P - \beta| - (P_y + G\alpha) = 0, \tag{5}$$

where G is the plastic modulus. The form of this function shows that kinematic hardening causes the elastic domain translation, while isotropic hardening causes the expansion of this domain. Figure 2 shows the expansion caused by the isotropic hardening in the load–internal hardening plane.

The irreversible nature of plastic flow is represented by means of the Kuhn–Tucker conditions [3]. Another constraint must be satisfied when $h(P, \alpha, \beta) = 0$. It is referred to as the *consistency condition* and corresponds to the physical requirement that a load point on the yield surface must persist on it [2]. These conditions are presented as follows:

$$\gamma \geqslant 0, \qquad \gamma h(P, \alpha, \beta) = 0, \qquad \gamma \dot{h}(P, \alpha, \beta) = 0 \quad \text{if } h(P, \alpha, \beta) = 0. \tag{6}$$

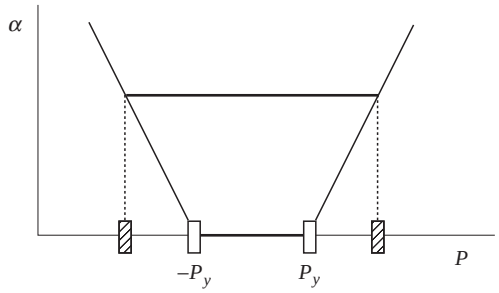

Figure 2. Elastic domain evolution in the load–internal hardening plane as a consequence of isotropic hardening.

3. ELASTO–PLASTIC OSCILLATOR

Considering a single-degree-of-freedom oscillator with mass m and an external linear viscous dissipation parameter c, the balance of linear momentum is expressed by the following equation:

$$m\ddot{x} + c\dot{x} + P(x, x^p, \alpha, \beta) = F(t), \tag{7}$$

where $P(x, x^P, \alpha, \beta)$ is the elasto–plastic restitution force of the oscillator and $F(t)$ is an external force.

If the variable $y = \dot{x}$ is defined, and a periodic excitation $F(t) = F_0 \sin(\Omega t)$ is considered, it is possible to write the following equations of motion using equations (1–4) for the restitution force. It must be noted that, by considering $X = (x, y, x^p, \alpha, \beta)$, the equations of motion have the form $\dot{X} = f(X, t)$, $X \in \mathscr{R}^5$, associated with complementary conditions (5, 6).

$$\begin{gathered}
\dot{x} = y, \qquad \dot{y} = \delta \sin(\Omega t) - c_0 y - \omega_0^2 (x - x^p), \qquad \dot{x}^p = \gamma \operatorname{sign}(P - \beta), \\
\dot{\alpha} = \gamma, \qquad \dot{\beta} = \gamma H \operatorname{sign}(P - \beta), \qquad h(P, \alpha, \beta) = |P - \beta| - (P_y + G\alpha), \gamma \geqslant 0, \\
\gamma h(P, \alpha, \beta) = 0, \qquad \gamma \dot{h}(P, \alpha, \beta) = 0 \quad \text{if } h(P, \alpha, \beta) = 0.
\end{gathered} \tag{8}$$

Here, $\delta = F_0/m$, $c_0 = c/m$ and $\omega_0^2 = K/m$.

4. EQUILIBRIUM POINTS

Considering free vibrations ($\delta = 0$), equilibrium points of the oscillator, $\bar{X}$, are defined when $f(\bar{X}) = 0$. Hence,

$$\bar{y} = \bar{\gamma} = 0, \qquad \bar{x} = x^p. \tag{9}$$

The system has only one equilibrium point which can vary continuously on the x-axis, since the plastic displacement, x^p, can do so. Another characteristic is that it occurs in the elastic region since $\bar{\gamma} = 0$ implies that $h(P, \alpha, \beta) \leqslant 0$.

Linearization of the equations of motion near the equilibrium point can be considered by defining a new variable $\eta = (\eta_1, \eta_2, \eta_3, \eta_4, \eta_5)$:

$$\eta = X - \bar{X}. \tag{10}$$

The linearization establishes that $\dot{\eta}_3 = \dot{\eta}_4 = \dot{\eta}_5 = 0$. Hence, η_3, η_4 and η_5 assume constant values. This behavior suggests a split in phase space in two parts. One part is called the *phase plane* and includes the variables x, y, or in the linearized problem the pair $\eta_p = (\eta_1, \eta_2)$. The other part is the *internal variables space* and includes x^p, α, β, or η_3, η_4, η_5 for linearized problem. Similar considerations apply to other dynamical systems. Savi and Braga [4] have studied the behavior of a shape memory oscillator with internal constraints using the same methodology.

With this assumption, the linearized system in the phase plane is treated as follows:

$$\dot{\eta}_p = [\mathbf{A}]\eta_p + b \quad \text{or} \quad \begin{Bmatrix} \dot{\eta}_1 \\ \dot{\eta}_2 \end{Bmatrix} = \begin{bmatrix} 0 & 1 \\ -\omega_0^2 & -c_0 \end{bmatrix} \begin{Bmatrix} \eta_1 \\ \eta_2 \end{Bmatrix} + \begin{Bmatrix} 0 \\ \omega_0^2 \eta_3 \end{Bmatrix}. \tag{11}$$

The behavior of the linearized system near the equilibrium point depends on the eigenvalues of matrix [**A**], which are

$$\lambda_{1,2} = -c_0/2 \pm i\sqrt{4\omega_0^2 - c_0^2}, \tag{12}$$

where $\mathrm{i} = \sqrt{-1}$.

If $c_0 = 0$, the equilibrium point represents a *center*, and if $c_0 \neq 0$, equation (12) represents a *stable spiral* [5].

It is important to observe that the dynamics of the linearized system near the equilibrium point was analyzed just from the phase plane, since the matrix [**A**] can be obtained from the linearization of this plane. No considerations about the internal variables space need be done to calculate the eigenvalues of [**A**]. The use of this procedure is very useful in the study of non-linear dynamics, since the geometric point of view is very important in chaotic dynamics analysis [5–10].

5. NUMERICAL PROCEDURE

The numerical solution procedure here proposed uses the operator split technique [11–13] to divide the space of variables into two parts. One part is the phase plane and includes the variables x, y and the other one is the internal variables space and includes x^p, α, β. This approach is similar to the one proposed in the preceding section which established a physical meaning for the operator split technique.

With the proposed split, it is possible to develop a numerical procedure using any integration scheme associated with the return mapping algorithm which consists of an elastic predictor step associated with a plastic corrector. An iterative process takes place until the convergence is achieved. The following sections present details on each part of the procedure.

5.1. TIME INTEGRATION

The time integration of equations of motion in the phase plane can be done by any integration scheme, since the internal variables x^p, α, β are considered as known parameters. As a first trial, an elastic predictor step is assumed, where the value of x^p, α, β remains constant from the previous time instant.

The next step of the solution procedure consists of a plastic corrector step. Hence, the feasibility of trial state is evaluated and the *return mapping algorithm* is considered [14].

5.2. RETURN MAPPING ALGORITHM

At this point, a trial state x_{n+1}, y_{n+1} is known. This is considered as an input for the return mapping algorithm. To present this algorithm, one first defines an auxiliary variable,

$$\zeta = P - \beta. \tag{13}$$

A trial state is defined by considering an elastic predictor step. Using the implicit Euler algorithm to time discretize the evolution equations (1–5), it is possible to write the following equations, which define the trial state:

$$P_{n+1}^{trial} = K(x_{n+1} - x_n^p), \qquad (x_{n+1}^p)^{trial} = x_n^p, \qquad \alpha_{n+1}^{trial} = \alpha_n, \tag{14–16}$$

$$\beta_{n+1}^{trial} = \beta_n, \qquad h_{n+1}^{trial} = |\zeta_{n+1}^{trial}| - (P_y - G\alpha_n). \tag{17, 18}$$

If $h_{n+1}^{trial} \leqslant 0$, it means that the state is in the elastic domain and the trial state is the actual one. Otherwise, if $h_{n+1}^{trial} > 0$, one is outside the elastic domain and a plastic step must be

considered. Hence, the trial state must be corrected. Simo and Taylor [14] have shown that the correction of the trial state must be done as follows:

$$P_{n+1} = P_{n+1}^{trial} - K\Delta\gamma \text{ sign } (\zeta_{n+1}^{trial}), \qquad x_{n+1}^{p} = (x_{n+1}^{p})^{trial} + \Delta\gamma \text{ sign } (\zeta_{n+1}^{trial}), \quad (19, 20)$$

$$\alpha_{n+1} = \alpha_{n+1}^{trial} + \Delta\gamma, \qquad \beta_{n+1} = \beta_{n+1}^{trial} + H\Delta\gamma \text{ sign } (\zeta_{n+1}^{trial}), \quad (21, 22)$$

where

$$\Delta\gamma = h_{n+1}^{trial}/(K + G + H). \quad (23)$$

5.3. ACTUAL STATE

Now, it is necessary to return to the phase plane equations and recalculate the variables using new values of the parameters x^p, α, β. This procedure must be repeated until it converges. This situation occurs when the difference between the actual and trial state reaches a prescribed tolerance.

6. NUMERICAL SIMULATIONS

This section presents some numerical simulations on the behavior of the elasto–plastic oscillator using the proposed procedure. Free and forced vibrations are considered for three different situations: kinematic, isotropic and kinematic/isotropic hardening.

The mid-point rule is used to perform the time integration of the phase plane equations. This procedure is unconditionally stable and introduces no spurious dissipation [2]. The same results can be obtained using the fourth order Runge–Kutta method. Good convergence is obtained for time steps, Δt, lower than $2\pi/(200\omega_0)$.

6.1. KINEMATIC HARDENING

This section is focused on the analysis of the elasto–plastic oscillator with kinematic hardening. Hence, isotropic hardening is neglected and the variable α is not considered. All simulations consider an oscillator with parameters presented in Table 1 and an unitary mass.

6.1.1 *Free Vibrations*

The free vibrations of the elasto–plastic oscillator are considered by letting δ vanish in equation (8). A system with no external dissipation ($c_0 = 0$) is considered. Results from simulations are presented in the form of phase portraits, where each orbit is associated with different initial conditions. Figure 3 shows the phase portrait in the phase plane (Figure 3(a)) and in the internal variables plane (Figure 3(b)). Initial conditions in the elastic domain cause linear responses. Outside the elastic domain, initial conditions cause a variation of the equilibrium point which is associated with plastic displacements. The phase portrait in the internal variables plane occupies a restricted region of the plane as a consequence of complementary conditions (6) (Figure 3(b)).

Figure 4 shows a particular orbit associated with initial conditions which are outside the elastic domain. The motion occurs around the equilibrium point whose position on

TABLE 1

Parameters of the oscillator with kinematic hardening

K (MN/m)	H (kN/m)	P_y (kN)
54·9	78·5	31·4

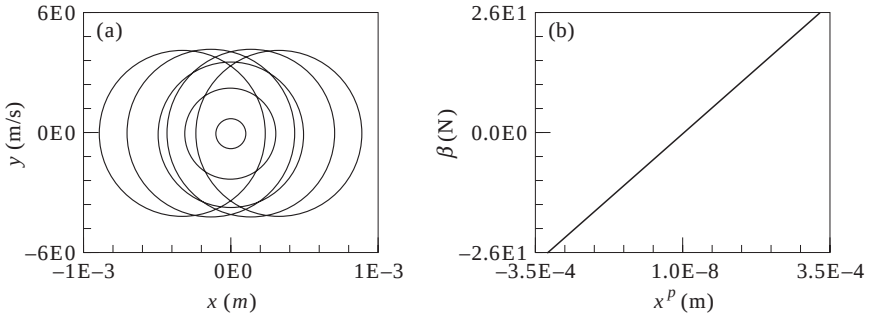

Figure 3. Phase portrait of the oscillator with kinematic hardening. (a) Phase plane, (b) internal variables plane.

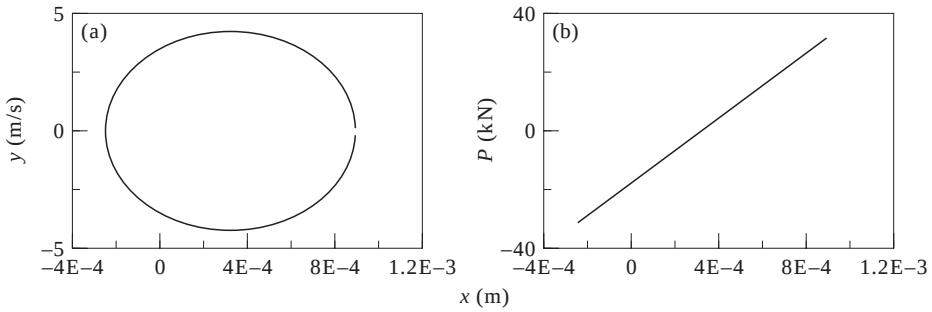

Figure 4. Response of the oscillator with kinematic hardening for a particular initial condition. (a) Phase plane, (b) force–displacement curve.

the x-axis is defined by the plastic displacement, x^p. Figure 4(a) shows the phase plane while Figure 4(b) shows the force–displacement curve.

The energy dissipation of the plastification process can be seen by considering an initial condition with a null displacement and a non-zero velocity. Figure 5 shows the response for $(x, y) = (0,6)$ and $(x^p, \beta) = (0,0)$. Figure 5(a) shows the phase plane while Figure 5(b) shows the load–displacement curve.

By considering an external dissipation, asymptotic behavior is expected. Figure 6 shows the phase plane and the displacement time history for a dissipation parameter $c_0 = 2000\ \mathrm{s}^{-1}$. The phase plane presents a stable spiral orbit that tends to the equilibrium point defined by the plastic displacement, x^p.

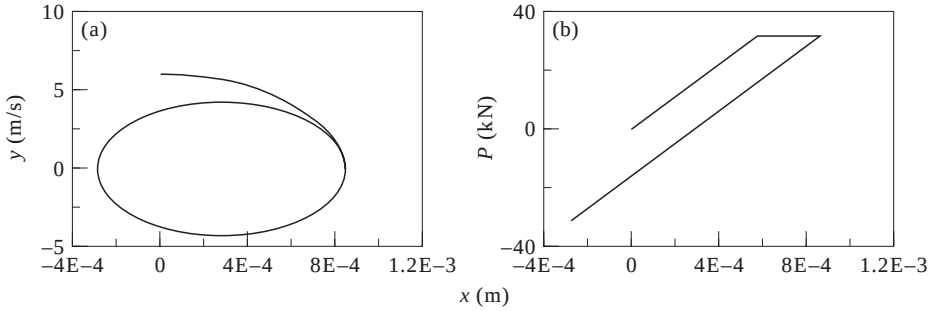

Figure 5. Energy dissipation during the plastification process in the oscillator with kinematic hardening. (a) Phase plane, (b) force–displacement curve.

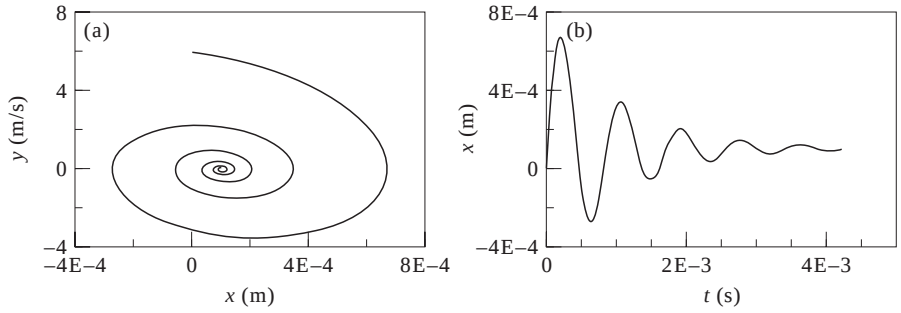

Figure 6. Response of the oscillator with kinematic hardening and external dissipation ($c_0 = 2000$ s^{-1}). (a) Phase plane, (b) displacement time history.

Free vibration numerical simulations agree with the analysis of linearized system (presented in section 4).

6.1.2. *Forced Vibrations*

In the forced vibration analysis it is clear that a forcing amplitude smaller than the elastic limit causes a linear response. Hence, one is interested in forcing amplitudes that cause plastic displacements. The elasto–plastic oscillator has two kinds of dissipation: an external linear viscous dissipation and an internal plastic dissipation. The effect of external dissipation is analyzed by considering different dissipation parameters: $c_0 = 0$ (with no external dissipation) and $c_0 = 2000\ \mathrm{s}^{-1}$. A forcing frequency $\Omega = 1000\ \mathrm{rads}^{-1}$ is considered for all simulations. The other parameters are identical to the one used in the free vibrations analysis.

Periodic excitation tends to cause a steady state response where plastic variables have a stabilized cycle. This is a consequence of kinematic hardening which imposes that the yield surface modifies its position. In the transient response, the translation of the yield surface causes a non-symmetric response for tensile and compressive behavior. In steady state response, a symmetric situation occurs and system variables present periodic responses.

Figure 7 shows the transient response for the first 30 loading cycles with $\delta = 41{\cdot}4\ K\ \mathrm{ms}^{-2}$, where no external dissipation is considered ($c_0 = 0$). A considerable amount of plastic displacements in the first cycles causes a high level of internal dissipation. This establishes that the initial transient response vanishes quickly and a stabilized elasto–plastic cyclic response is observed after a few cycles of loading. Figures 7(a–d) show the time history of displacement, velocity, plastic displacement and back load, respectively, while Figure 7(e) shows the load–displacement curve. In Figure 8, the phase plane for the first 100 cycles shows a small drift in orbits position until a steady state response is reached.

When external dissipation is considered, the system response presents smaller displacement in the first cycles. This behavior causes a decrease of plastic displacements in these first cycles and, as a consequence, smaller energy dissipation is present. Furthermore, the transient response is longer than the previous case. It is possible to see this behavior by comparing the variables stabilization of both cases, presented in Figures 7, 8 and Figures 9, 10, respectively.

In the foregoing analysis, steady state responses are considered. Figures 11–14 show phase plane, load-displacement curve, time history and the Fast Fourier Transform (FFT) of displacement for different driving force amplitudes.

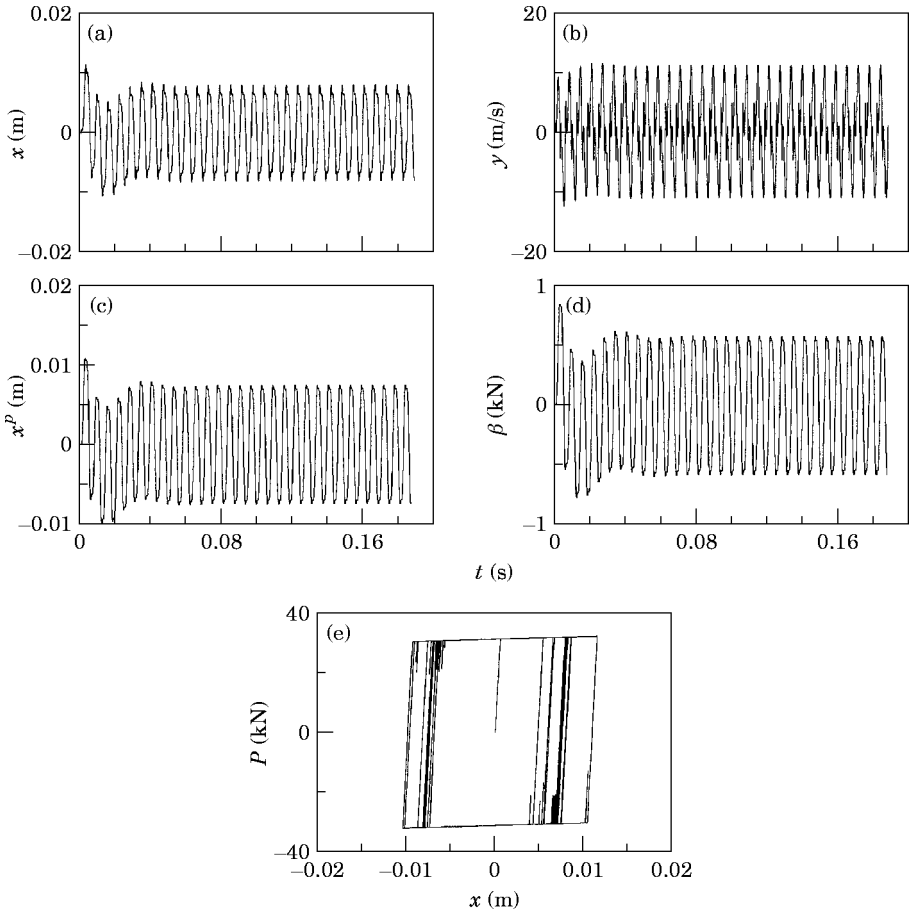

Figure 7. Behavior of the oscillator with kinematic hardening and no external dissipation. (a) Displacement time history, (b) velocity time history, (c) plastic displacement time history, (d) back load time history, (e) load–displacement curve.

Figure 11 shows the oscillator response for $\delta = 31{\cdot}4\ K\ \mathrm{ms}^{-2}$. FFT analysis shows that response and forcing frequency are the same. When increasing the driving force amplitude, a superharmonic response is present. Figures 12–14 show the oscillator response for

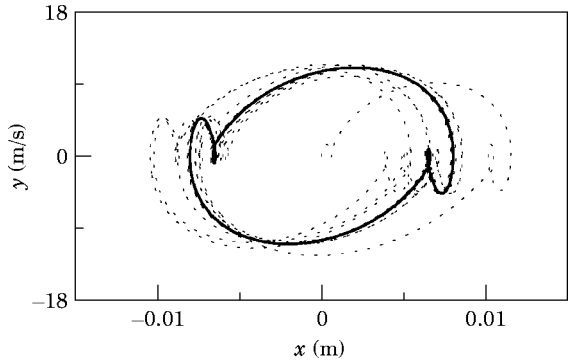

Figure 8. Phase plane orbits of the oscillator with kinematic hardening and no external dissipation for the first 100 loading cycles: —, 100th cycle; ----, evolution of the orbits.

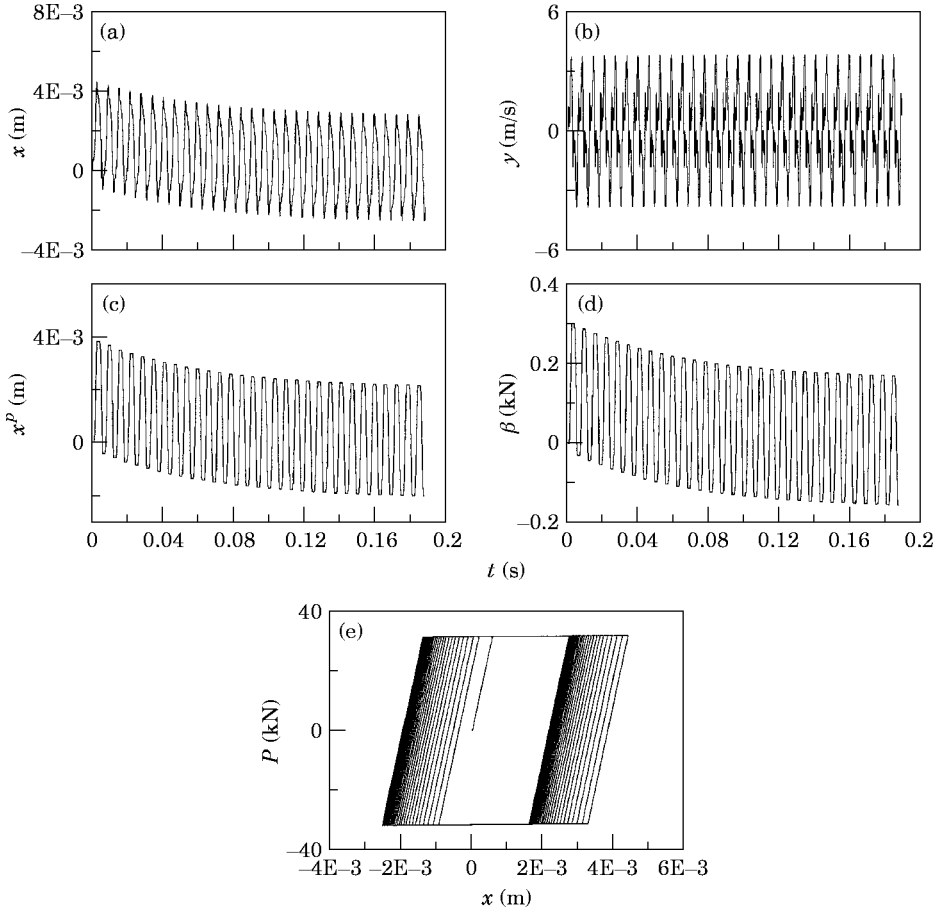

Figure 9. Behavior of the oscillator with kinematic hardening and external dissipation. (a) Displacement time history, (b) velocity time history, (c) plastic displacement time history, (d) back load time history, (e) load–displacement curve.

$\delta = 41{\cdot}4\ K\ \mathrm{ms}^{-2}$, $\delta = 51{\cdot}4\ K\ \mathrm{ms}^{-2}$ and $\delta = 61{\cdot}4\ K\ \mathrm{ms}^{-2}$, respectively. FFT analysis of the displacement signal showed that the superharmonic response is associated with odd multiples of the forcing frequency.

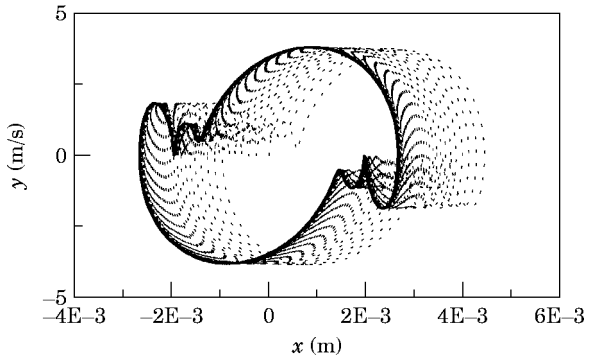

Figure 10. Phase plane orbits of the oscillator with kinematic hardening and external dissipation for the first loading cycles: —, 100th cycle;----, evolution of the orbits.

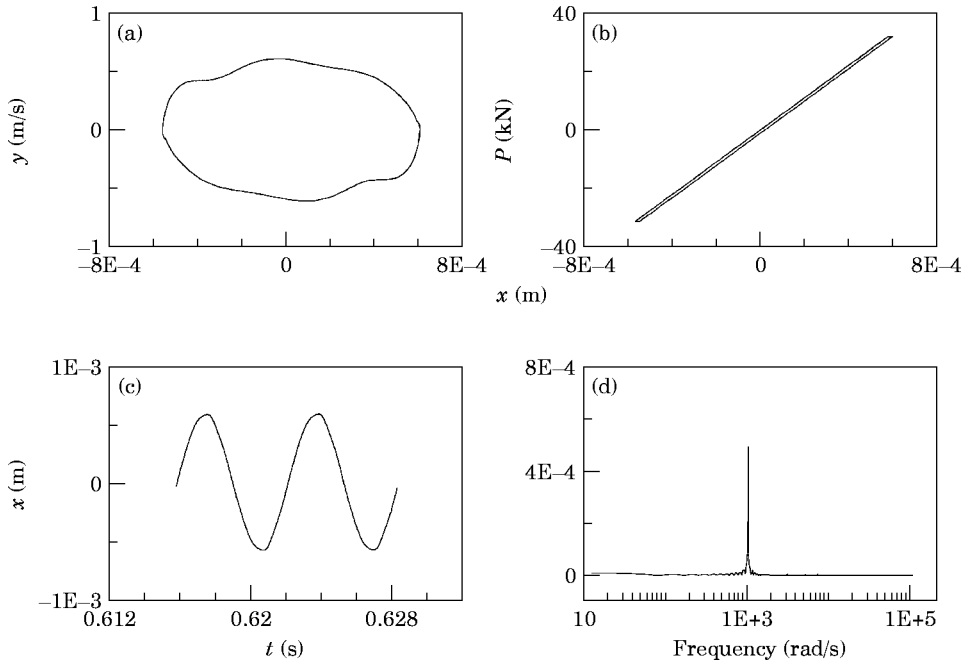

Figure 11. Steady state response of the oscillator with kinematic hardening for $\delta = 31{\cdot}4\ K\ \mathrm{ms}^{-2}$. (a) Phase plane, (b) load–displacement curve, (c) displacement steady state response, (d) displacement frequency response.

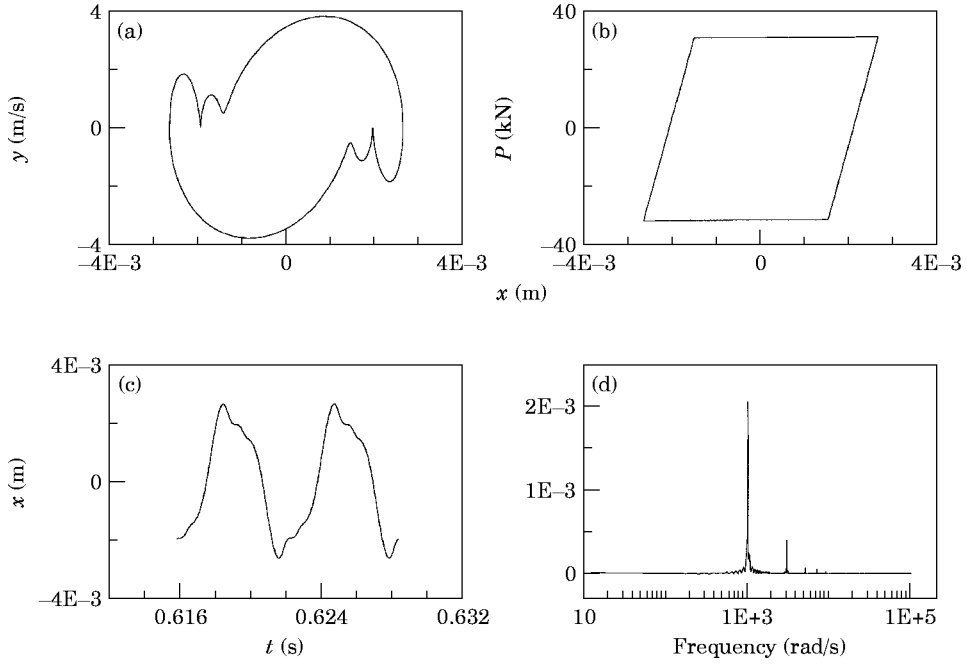

Figure 12. Steady state response of the oscillator with kinematic hardening for $\delta = 41{\cdot}4\ K\ \mathrm{ms}^{-2}$. (a) Phase plane, (b) load–displacement curve, (c) displacement steady state response, (d) displacement frequency response.

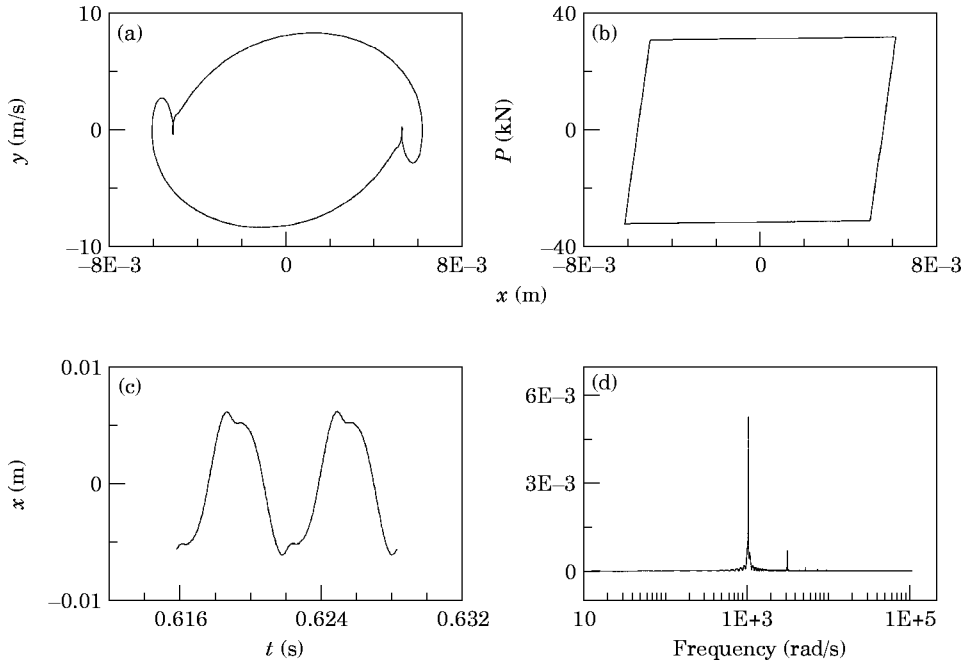

Figure 13. Steady state response of the oscillator with kinematic hardening for $\delta = 51{\cdot}4\ K\ \mathrm{ms}^{-2}$. (a) Phase plane, (b) load–displacement curve, (c) displacement steady state response, (d) displacement frequency response.

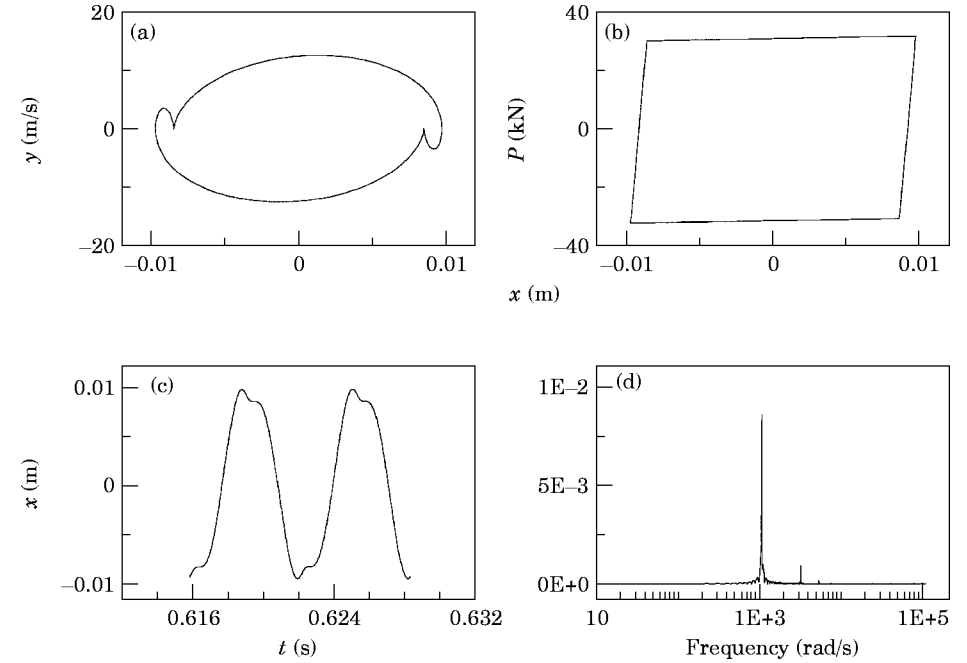

Figure 14. Steady state response of the oscillator with kinematic hardening for $\delta = 61{\cdot}4\ K\ \mathrm{ms}^{-2}$. (a) Phase plane, (b) load–displacement curve, (c) displacement steady state response, (d) displacement frequency response.

TABLE 2

Parameters of the oscillator with isotropic hardening

K (MN/m)	G (N/m)	P_y (kN)
54·9	345·6	31·4

6.2. ISOTROPIC HARDENING

This section is focused on the analysis of an elasto–plastic oscillator with isotropic hardening. Hence, kinematic hardening is neglected and the variable β is not considered. All simulations consider an oscillator with parameters presented in Table 2 and a unitary mass.

6.2.1 *Free Vibrations*

Free vibrations of an elasto–plastic oscillator with kinematic and with isotropic hardening are similar. The phase portrait in the phase plane is shown in Figure 15(a). Figure 15(b) shows the phase portrait in the internal variables plane where it is possible to see that a restricted region of the plane is occupied as a consequence of the complementary conditions (6). Since the yield surface expands, the parameter α is always positive.

6.2.2 *Forced Vibrations*

The behavior of an elasto–plastic oscillator with periodic excitation is now considered with a forcing frequency $\Omega = 1000$ rads^{-1} and an amplitude $\delta = 41{\cdot}4\ K$ ms^{-2}. It is assumed that the other parameters are identical to the one used in the free vibrations analysis. By prescribing loads, isotropic hardening tends to cause an elastic stabilized response in steady state. It is a different behavior from the one obtained by the oscillator with kinematic hardening where a stabilized elasto-plastic response occurs.

Figure 16 shows the transient response for the first 30 loading cycles, where no external dissipation is considered ($c_0 = 0$). Steady state is reached after a few cycles. This situation is similar to the one presented by the oscillator with kinematic hardening. Figures 16(a, b) show the time history of displacement and velocity. The initial superharmonic response can be observed which is caused by the cyclic response of the plastic displacements.

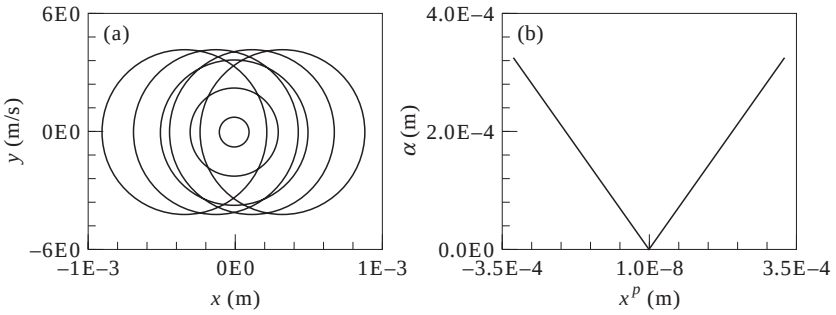

Figure 15. Phase portrait of the oscillator with isotropic hardening. (a) Phase plane, (b) internal variables plane.

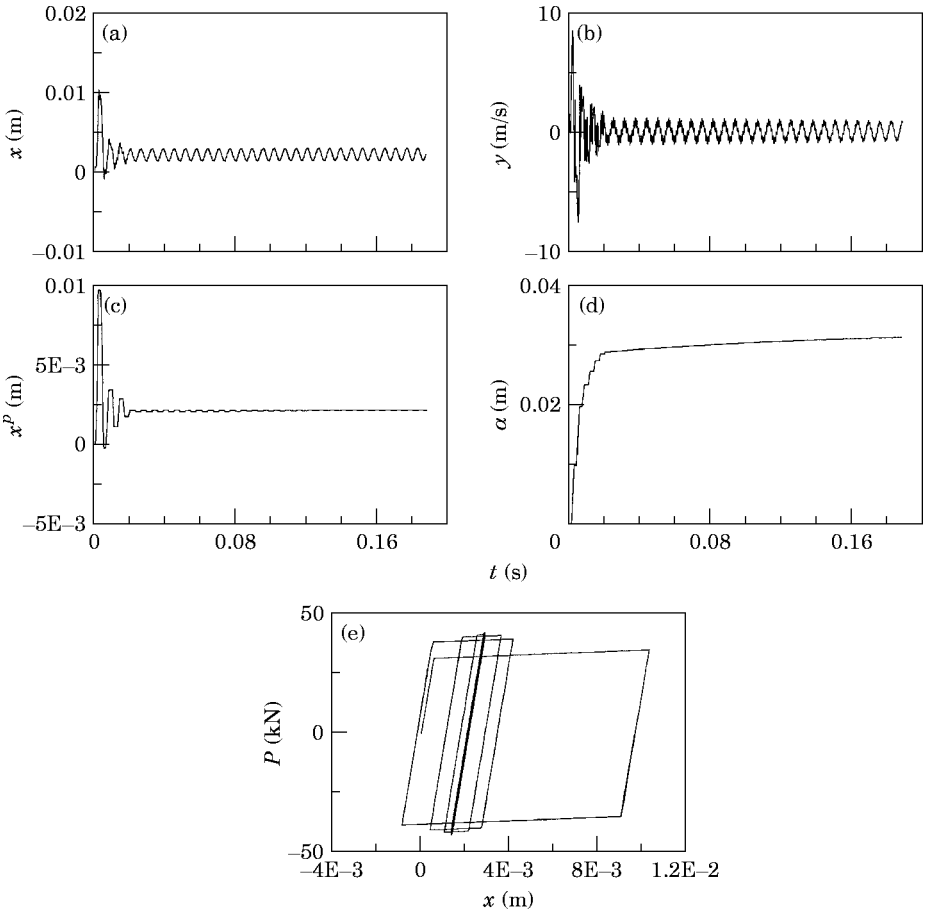

Figure 16. Behavior of the oscillator with isotropic hardening and no external dissipation. (a) Displacement time history, (b) velocity time history, (c) plastic displacement time history, (d) internal hardening time history, (e) load–displacement curve.

Figure 16(c) shows the time history of plastic displacement while the internal hardening variable stabilization is observed in Figure 16(d). The load–displacement curve is presented in Figure 16(e).

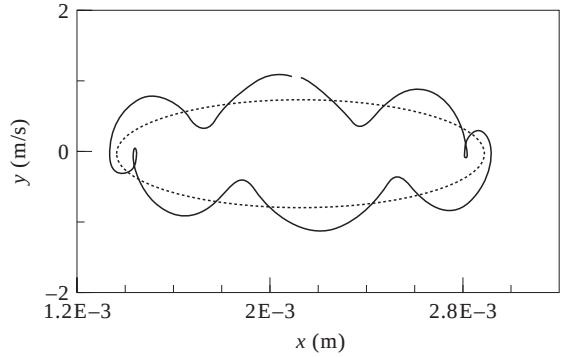

Figure 17. Phase plane orbits of the oscillator with isotropic hardening and no external dissipation for the 10th (—) and 100th (----) loading cycle.

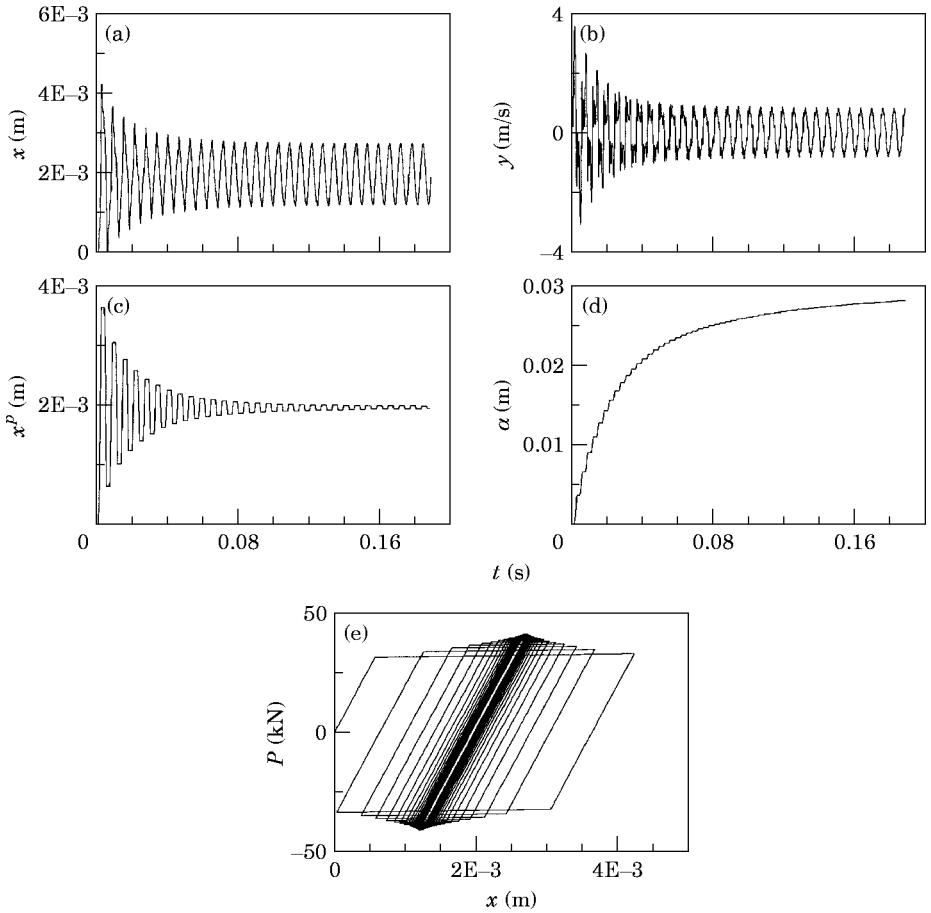

Figure 18. Behavior of the oscillator with isotropic hardening and external dissipation. (a) Displacement time history, (b) velocity–time history, (c) plastic displacement time history, (d) internal hardening time history, (e) load-displacement curve.

When steady state is reached, there is an elastic response where plastic displacements assume constant values while displacement and velocity present a periodic response. In the phase plane, the orbits tend to an elliptical shape. Figure 17 shows different forms of orbits for the 10th and 100th cycle.

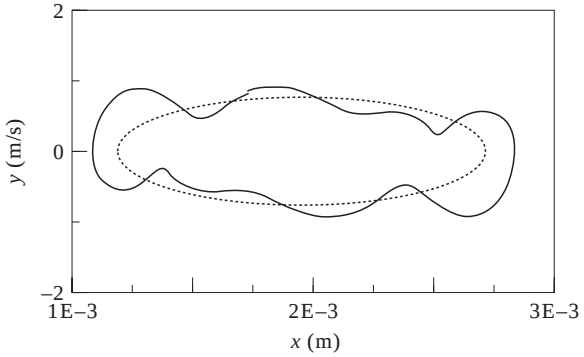

Figure 19. Phase plane orbits of the oscillator with isotropic hardening and external dissipation for the 10th (—) and 100th (----) loading cycle.

TABLE 3

Parameters of the oscillator with kinematic/isotropic hardening

K (MN/m)	G (kN/m)	H (kN/m)	P_y (kN)
54·9	345·6	78.5	31·4

As in the case with kinematic hardening, by considering external dissipation, the system response presents a reduction of plastic displacements in the first cycles. This implies an internal dissipation decrease and a longer transient response is expected (Figure 18).

Figure 19 shows different forms of phase plane orbits for the 10th and 100th loading cycles. Again, the orbits tend to an elliptical shape.

6.3. KINEMATIC AND ISOTROPIC HARDENING

In this section, an analysis of an elasto–plastic oscillator with a combination of kinematic and isotropic hardening is considered. All simulations consider an oscillator with parameters presented in Table 3 and a unitary mass.

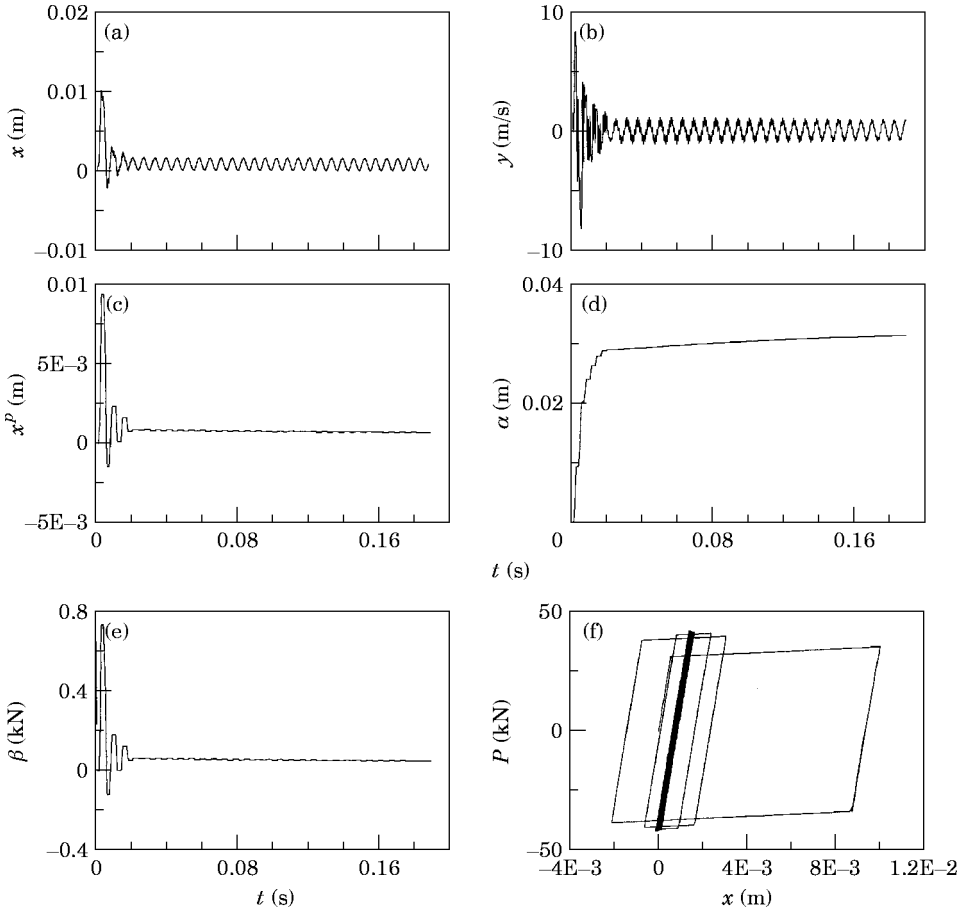

Figure 20. Behavior of the oscillator with kinematic/isotropic hardening and no external dissipation. (a) Displacement time history, (b) velocity time history, (c) plastic displacement time history, (d) internal hardening time history, (e) back load time history, (f) load–displacement curve.

The free vibrations present the same behavior as the one observed in kinematic or isotropic hardening. Hence, the following analysis is dedicated to the force vibration problem. A forcing frequency $\Omega = 1000$ rads^{-1} and an amplitude $\delta = 41{\cdot}4\,K$ ms^{-2} is considered.

Since isotropic hardening tends to expand the yield surface and the loads are prescribed, it is expected that the oscillator with kinematic/isotropic hardening presents an elastic response in steady state, as it is observed in the response of an oscillator with isotropic hardening (kinematic hardening is neglected).

Figure 20 shows the transient response for the first 30 loading cycles, where no external dissipation is considered ($c_0 = 0$). Figures 20(a, b) show the time history of displacement and velocity. The initial superharmonic response is shown which is caused by the cyclic response of plastic displacements. As it is expected, the internal hardening variable, α, tends to assume a constant value (Figure 20(d)). Constant values are also assumed for the plastic displacement (Figure 20(c)) and the back load, β (Figure 20(e)), by a different way that occurs when isotropic hardening is neglected. Figure 20(f) shows the load–displacement curve. Since no external dissipation is considered, the initial transient response vanishes quickly as a consequence of the high level of internal dissipation in the first cycles.

Orbits in the phase plane tend to modify their form and position until steady state is reached when an elliptical shape is assumed. Figure 21 shows different orbits for the 10th and 100th cycle. When steady state is reached, plastic displacements assume constant values while displacement and velocity present the periodic response.

When external dissipation is considered, a reduction of displacement amplitudes in the first cycles takes place. This behavior tends to reduce internal dissipation causing a longer transient response (Figure 22), as observed in the response of the oscillator with kinematic or with isotropic hardening.

Phase plane orbits show, in a more drastic form, the response evolution due to the combination of kinematic an isotropic hardening. Figure 23 shows different orbits for the 10th and 100th cycle.

Now, the frequency analysis is focused. One is interested in the effects of forcing frequency variation on the oscillator steady state response. A system with no external dissipation is considered. Figure 24 shows the behavior of the x-range, $\Delta x = x_{max} - x_{min}$, and the internal hardening variable, α, under the variation of forcing frequency. Similar qualitative behavior may be observed in both cases. The response amplification, typical behavior of system response under resonant conditions, can be observed when

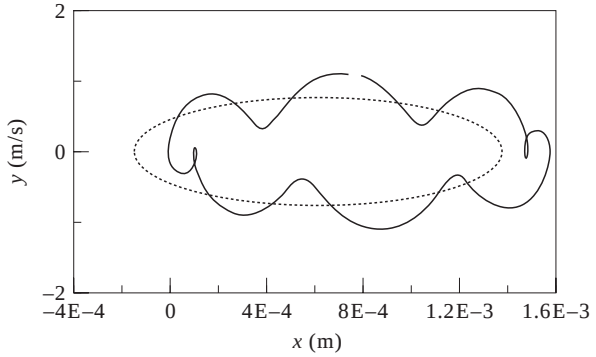

Figure 21. Phase plane orbits of the oscillator with kinematic/isotropic hardening and no external dissipation of the 10th (—) and 100th (----) loading cycle.

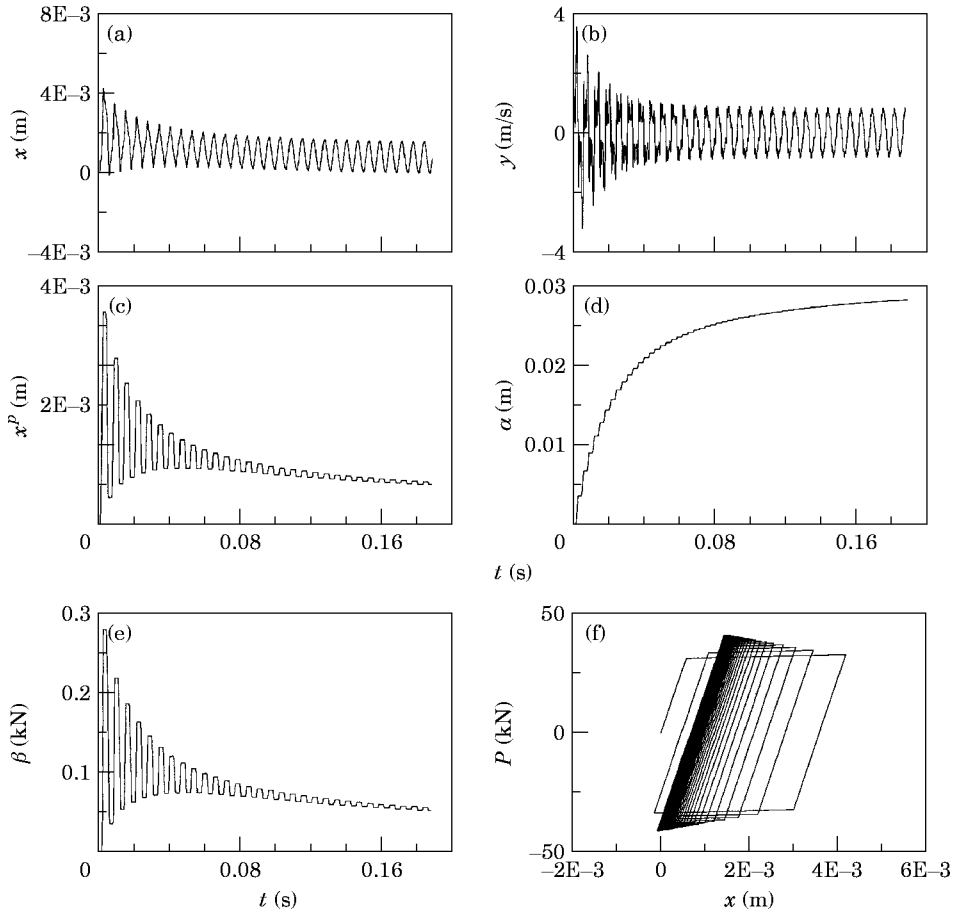

Figure 22. Behavior of the oscillator with kinematic/isotropic hardening and external dissipation. (a) Displacement time history, (b) velocity time history, (c) plastic displacement time history, (d) internal hardening time history, (e) back load time history, (f) load–displacement curve.

$6400 < \Omega < 6800$ rads^{-1}. Since the elastic natural frequency is approximately 7400 rads^{-1}, it is clear that the plastic effect tends to reduce the resonant frequency as it is observed when external dissipation is considered.

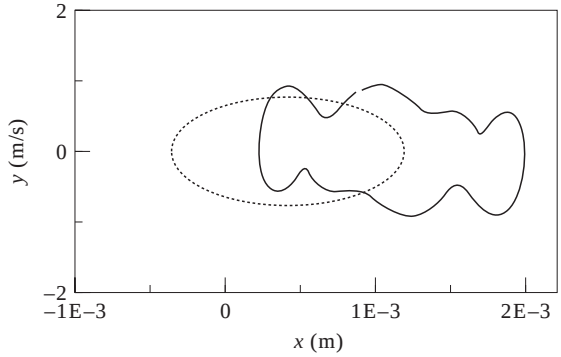

Figure 23. Phase plane orbits of the oscillator with kinematic/isotropic hardening and external dissipation for the 10th (—) and 100th (----) loading cycle.

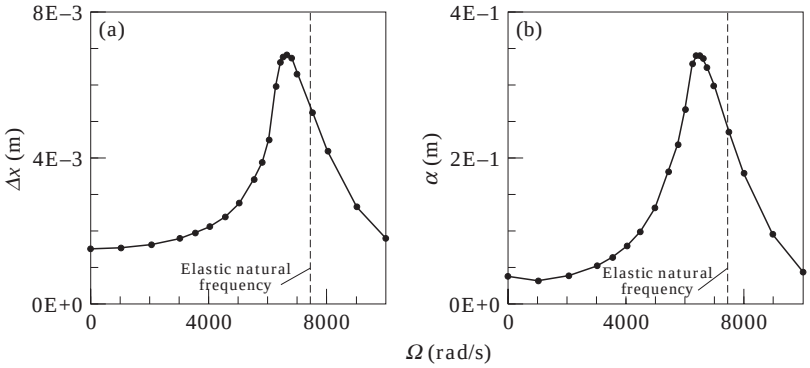

Figure 24. Frequency response for $\delta = 41{\cdot}4\ K\,\mathrm{ms}^{-2}$: (a) Δx, (b) α.

7. CONCLUSIONS

A dynamic analysis of an elasto-plastic oscillator with kinematic and isotropic hardening was performed. Despite the deceiving simplicity of the model used, its non-linear dynamic reponse may represent the qualitative response of general elasto-plastic structures. The equations of motion have five state variables associated with the complementary conditions. An analysis of equilibrium points suggest a split in phase space variables. This procedure allows one to analyze the dynamics of a 5-dimensional system by considering just a part of the space of state variables. The space split is in close agreement with the operator split technique used in the numerical solution of equations of motion. The numerical method proposed in this work permits the use of a combination of classical algorithms to evaluate the response of elasto-plastic dynamical systems. Good convergence is achieved using relatively large time steps. The periodic forcing response of an elasto–plastic oscillator is considered for different hardening effects. Kinematic hardening may cause a superharmonic steady state response where plastic variables assume periodic responses. Isotropic hardening has an elastic steady state response where plastic variables assume constant values. The combination of kinematic and isotropic hardening also presents an elastic steady state response. By considering no external dissipation, a considerable amount of plastic displacement in the first cycles causes high level of internal dissipation, which establishes that the initial transient response vanishes quickly. On the other hand, when an external linear viscous dissipation is considered, a reduction of the displacement amplitudes in the first cycles results. It tends to reduce internal dissipation causing a longer transient response. Frequency analysis shows that the elasto-plastic resonant frequency is lower than the elastic natural frequency. This conclusion can be obtained by evaluating the response amplification of the x-range or internal hardening variable to the variation of forcing frequency.

REFERENCES

1. R. Hill 1950 *The Mathematical Theory of Plasticity*. Oxford: Clarendon.
2. J. C. Simo 1994 *Topics on the Numerical Analysis and Simulation of Plasticity*. Handbook of Numerical Analysis.
3. D. G. Luenberger 1973 *Introduction to Linear and Nonlinear Programming*. Reading: Addison-Wesley.
4. M. A. Savi and A. M. B. Braga 1993 *Proceedings of the* 12*th Brazilian Congress of Mechanical Engineering*, University of Brasília, Brazil, Chaotic response of a shape memory oscillator with internal constraints.

5. F. MOON 1987 *Chaotic Vibrations*. New York: John Wiley.
6. J. GUCKENHEIMER and P. HOLMES 1983 *Nonlinear Oscillations, Dynamical Systems, and Bifurcations of Vector Fields*. New York: Springer-Verlag.
7. T. MULLIN 1993 *The Nature of Chaos*. New York: Oxford Press.
8. E. OTT 1993 *Chaos in Dynamical Systems*. New York: Cambridge Press.
9. J. M. T. THOMPSON and H. B. STEWART 1986 *Nonlinear Dynamics and Chaos*. Chichester: John Wiley.
10. S. WIGGINS 1990 *Introduction to Applied Nonlinear Dynamical Systems and Chaos*. New York: Springer-Verlag.
11. A. CHORIN, T. J. R. HUGHES, M. F. MCCRACKEN and J. E. MARSDEN 1978 *Communications in Pure and Applied Mathematics* **31**, 205–256. Product formulas and numerical algorithms.
12. M. ORTIZ, P. M. PINSKY and R. L. TAYLOR 1983 *Computer Methods in Applied Mechanical Engineering* **39**, 137–157. Operator split methods for the numerical solution of the elastoplastic dynamic problem.
13. G. L. MARCHUCK 1975 *Methods of Numerical Analysis*. New York: Springer-Verlag.
14. J. C. SIMO and R. L. TAYLOR 1985 *Computer Methods in Applied Mechanical Engineering* **48**, 101–118, Consistent tangent operators for rate-independent elastoplasticity.